



## Band 7 Polarization Morphology of VLA 1623

None Assigned

### ABSTRACT

Magnetic fields have long been thought to be the primary driver of dust-grain polarization within circumstellar disks, although observations which effectively constrain the disk magnetic field are rare. Polarization morphology in the multiple system VLA 1623 has shown evidence of a magnetic field in multiple ALMA bands. Specifically, polarization morphology is remarkably consistent in bands 4, 5, and 6, with polarization degree increasing with wavelength, both of which are signs of magnetic field alignment. However, recent observations of the circumbinary disk surrounding L1448-IRS3B have highlighted the presence of mechanical dust-grain alignment, as polarization angles are well aligned with the spiral arms of the disk. To better constrain the polarization mechanism and small-scale structure within VLA 1623's circumbinary disk, we propose high-resolution polarization-mode Band 7 observations. If the polarization mechanism is determined to be mechanical alignment, we will gain new information on dust-grain shape, aspect ratio, and optical depth. If magnetic alignment is prevalent, we can further constrain the properties of the magnetic field and the strength of its components.

|   |  |                            |       |                           |       |
|---|--|----------------------------|-------|---------------------------|-------|
| <b>SCIENCE CATEGORY:</b>                    | Circumstellar disks, exoplanets and the solar system |                            |       |                           |       |
| <b>ESTIMATED 12-M TIME:</b>                 | 31.1 h   | <b>ESTIMATED 7-M TIME:</b> | 0.0 h | <b>ESTIMATED TP TIME:</b> | 0.0 h |
| <b>DUPLICATE OBSERVATION JUSTIFICATION:</b> |  |                            |       |                           |       |

### REPRESENTATIVE SCIENCE GOALS (UP TO FIRST 30)

| SCIENCE GOAL              | CLUSTER      | POSITION (ICRS)     | BAND | ANG.RES.('') | LAS.('') | 12m time (hrs) | 7m time (hrs) | TP time (hrs) | Number of sources |
|---------------------------|--------------|---------------------|------|--------------|----------|----------------|---------------|---------------|-------------------|
| Science Goal              | Science Goal | 16:26:26, -24:24:29 | 7    | 0.040        | 0.200    | 31.1           | N/A           | N/A           | 1                 |
| Total # Science Goals : 1 |              |                     |      |              |          |                |               |               |                   |

|                                    |      |                                    |    |                        |    |
|------------------------------------|------|------------------------------------|----|------------------------|----|
| <b>SCHEDULING TIME CONSTRAINTS</b> | NONE | <b>TIME ESTIMATES OVERRIDDEN ?</b> | No | <b>JOINT PROPOSAL?</b> | No |
|------------------------------------|------|------------------------------------|----|------------------------|----|

## 1 Scientific Justification

Circumbinary disks naturally lend themselves to complicated polarization structure due to their complex morphologies (e.g. L1448-IRS3B (priv. comm.)). These objects present unique environments for studying dust-grain polarization, and thus allow for the characterization of multiple polarization mechanisms. Prior studies have claimed that polarization in circumbinary disks is primarily driven by dust-grain alignment with magnetic fields (e.g. BHB 07-11 (Alves et al., 2018), VLA 1623 ((Sadavoy et al., 2018a), IRAS 16293-2422 (Sadavoy et al., 2018b)). Recent high-resolution ALMA observations of the circumbinary disks in L1448-IRS3B and BHB 07-11, however, have indicated that mechanical dust-grain alignment may be the prevalent polarization mechanism over magnetic fields. Hoang et al. (2022) suggests that mechanical alignment is dependent on the angular momentum and of the dust-grain as well as its iron inclusion properties. New studies propose that such alignment does not require angular momentum, and is instead based upon the shape and size of the dust-grains (Lin et al., 2024). Because a limited amount of high-resolution polarization mode observations of circumbinary disks exist, it is difficult to further study and constrain these proposed mechanisms. Additionally, it is difficult to differentiate mechanical alignment from that driven by magnetic fields. **To build upon our sample of circumbinary disks, we propose a series of high-resolution polarization mode observations of the VLA 1623 circumbinary disk, which will provide further insight into the proposed mechanical alignment mechanisms, as well as the observational differences between mechanical alignment and magnetic field alignment.**

## 2 VLA 1623

VLA 1623 is a Class 0 hierarchical multiple star system, with sources VLA 1623-A and VLA 1623-B in a close binary, and a third source VLA 1623-W separated by approximately  $10''$  to the west (Sadavoy et al., 2024). Additionally, VLA 1623-A itself is a compact binary system, with its constituent sources *Aa* and *Ab* maintaining a separation of approximately 14 au (Harris et al., 2018)(Fig. 1, left). The VLA 1623-A system is encompassed by a large circumbinary disk, which shows Keplerian rotation out to  $\sim 150$  au (Sadavoy et al., 2024; Murillo et al., 2013).

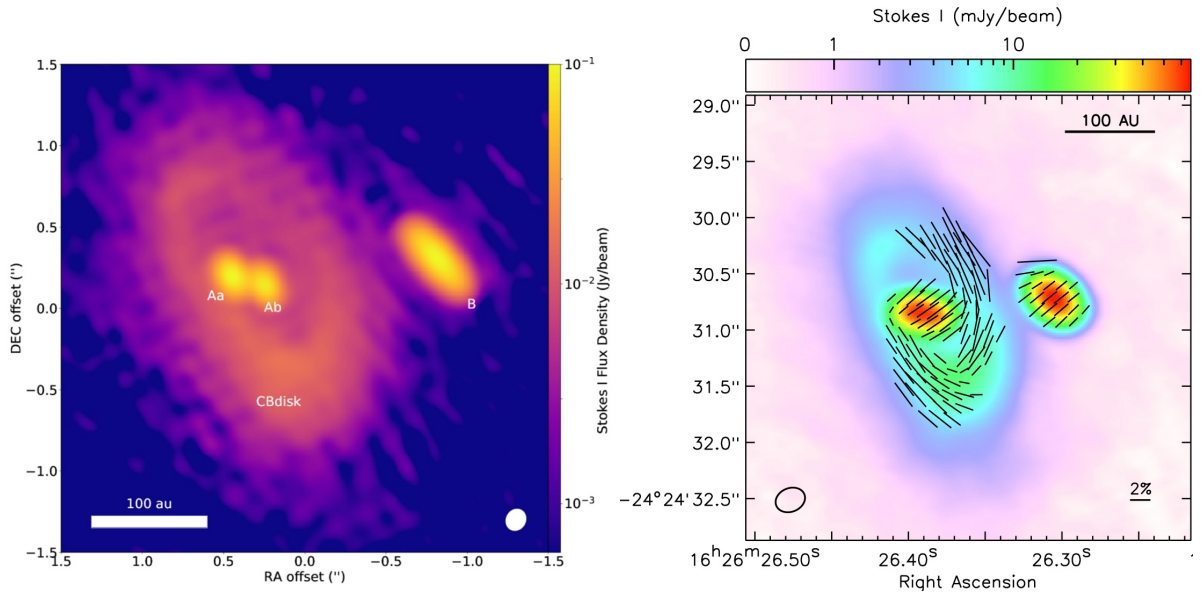


Figure 1: Left: An ALMA 872  $\mu\text{m}$  dust continuum Stokes I map of the VLA 1623-A and VLA 1623-B system. The compact binary sources *Aa* and *Ab* are resolved in the eastern portion of the system (Fig. 3 in Harris et al. (2018)). Right: An ALMA Band 6 map of Stokes I emission with polarization angles overlaid in black. Polarization vectors are scaled by polarization intensity (Fig. 3 in Sadavoy et al. (2018a)).

VLA 1623 has been observed with ALMA bands 4, 5, and 6 in full polarization mode at  $\sim 0.3'' - 0.5''$ . The observed polarization morphology is remarkably consistent across these three bands. Polarization angles align radially at small scales, and azimuthal alignment is prevalent throughout the larger circumbinary disk (Fig. 1, right) (Sadavoy et al., 2018a). The small-scale alignment indicates dust self-scattering in the circumstellar disks of VLA 1623-A and B, as the polarization fraction throughout the disks is less than 3% and the observed polarization angles are aligned along the disk minor axis (Sadavoy et al., 2018a). Based on the aforementioned Band 6 observations, Sadavoy et al. (2018b) determined that polarization in the circumbinary disk is likely due to grain alignment in a magnetic field. Specifically, the paper claims that a radial magnetic field with minute curvature (i.e., an hourglass) is responsible for the observed polarization morphology. However, recent high-resolution observations of multiple Class 0/I circumbinary systems shed light on the possibility of mechanical dust-grain alignment. Similar large-scale polarization morphology is also seen in L1448-IRS3B and BHB 07-11, which are the two best candidates of mechanically driven dust-grain polarization to date.

### 3 Mechanically Induced Polarization

Keplerian rotation has been linked to mechanical dust grain alignment in optically thin regions of circumstellar disks, particularly in long wavelength ALMA bands (e.g., Stephens et al., 2023; Lin et al., 2024). Polarization angles form an elliptical "bullseye" pattern (i.e., azimuthal alignment) with polarization fractions of up to 10%. In the circumbinary disks of L1448-IRS3B and BHB 07-11 (discussed below), this effect is also appears to be prevalent. However, rather than displaying alignment through Keplerian rotation, dust grains appear to be aligned with spiral structures within the disk. We believe that this effect may also be prevalent in VLA 1623.

#### 3.1 L1448-IRS3B

Like VLA 1623, L1448-IRS3B is a hierarchical Class 0 system with a prevalent circum-multiple disk. Sources *a* and *b* orbit in a close binary with separation  $\sim 75$  au, while source *c* resides  $\sim 230$  au to the east (Fig. 2, left) (Reynolds et al., 2021). The disk shows Keplerian rotation out to large scales, and indicates the kinematic center of the system to be near source *a*. (Reynolds et al., 2021) estimates the masses of *a* and *b* to be  $\sim 0.56 M_{\odot}$ , and *c* to be  $< 0.2 M_{\odot}$ .

High-resolution, polarization-mode Band 4 and 7 observations of L1448-IRS3B show multiple polarization mechanisms present throughout the disk (priv. comm.) (Fig. 2, right). Polarization angles are aligned at  $\sim 45^{\circ}$  in the outer regions of the disk, which is consistent with a magnetic field at envelope scales (priv. comm.). On circumstellar disk scales, polarization morphology and intensity indicates that dust self-scattering is the dominant polarization mechanism. Throughout the spiral arms, polarization angles are aligned with the gas flows. As such, these regions serve as the primary targets for studying mechanical dust-grain alignment.

#### 3.2 BHB 07-11

In addition to L1448-IRS3B, the circumbinary disk of BHB 07-11, a binary Class I protostellar system, serves as an environment for studying mechanical dust-grain polarization. The disk shows Keplerian motion throughout, and the defined spiral arms make BHB 07-11 the best candidate for studying mechanical dust-grain polarization (Alves et al. (2017), priv. comm.).

BHB 07-11 has been observed with ALMA bands 3, 6, and 7 in full polarization-mode at  $\sim 0.1'' - 0.15''$ . Polarization morphology is consistent in each band, and traces an azimuthal pattern which encompasses BHB 07-11's constituent sources (VLA 5a and VLA 5b) (Alves et al., 2018). Additionally, high-resolution ( $0.03''$ ) non-polarization-mode Band 6 continuum observations reveal complex spiral arm morphology at  $\sim 100$  au scales (Fig. 3, left). Polarization angles are well aligned with the spiral arms, suggesting that mechanical dust-grain alignment may be prevalent in these structures (Fig. 3, right). Alves et al. (2018) claims that a rotating magnetic field with a

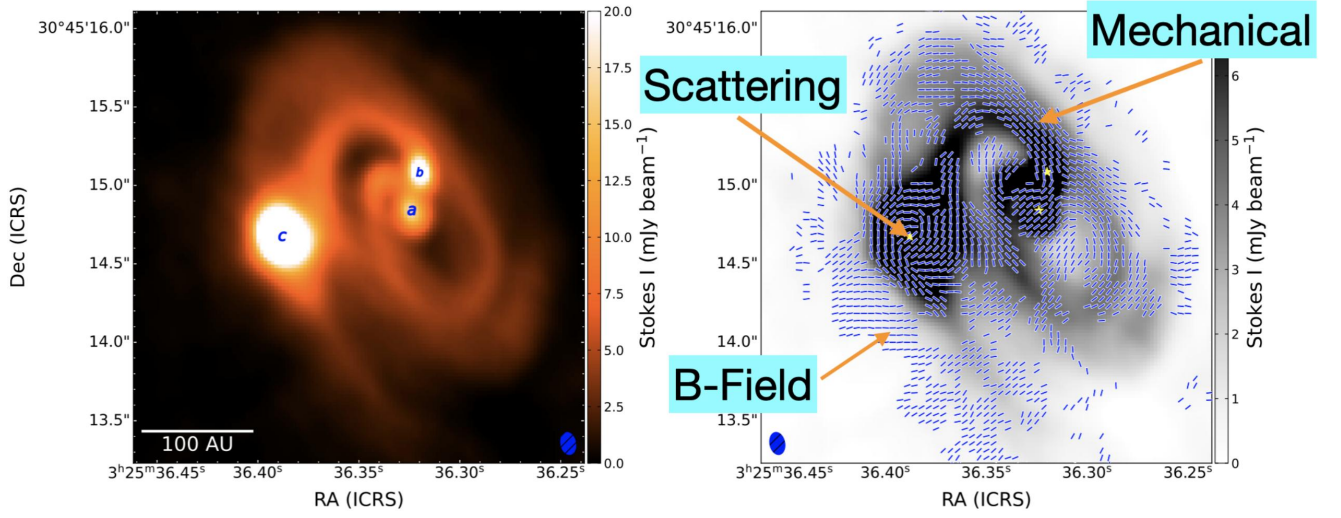


Figure 2: Left: An ALMA Band 7 Stokes I map of L1448-IRS3B with sources *a*, *b*, and *c* labeled (priv. comm.). Right: ALMA Band 7 polarization angles overlaid on a Stokes I map. Polarization vectors maintain the same length to highlight different alignment mechanisms (priv. comm.).

3:1 poloidal to toroidal strength ratio is responsible for the dust-grain alignment. While BHB 07-11 displays strong evidence for magnetic field alignment, it is difficult to discount the polarization angle alignment within the spiral arms. Additionally, high-resolution (0.04") polarization-mode Band 7 observations were proposed during the previous ALMA cycle. These observations will provide additional information regarding polarization morphology in the spiral arms and mechanical dust-grain alignment.

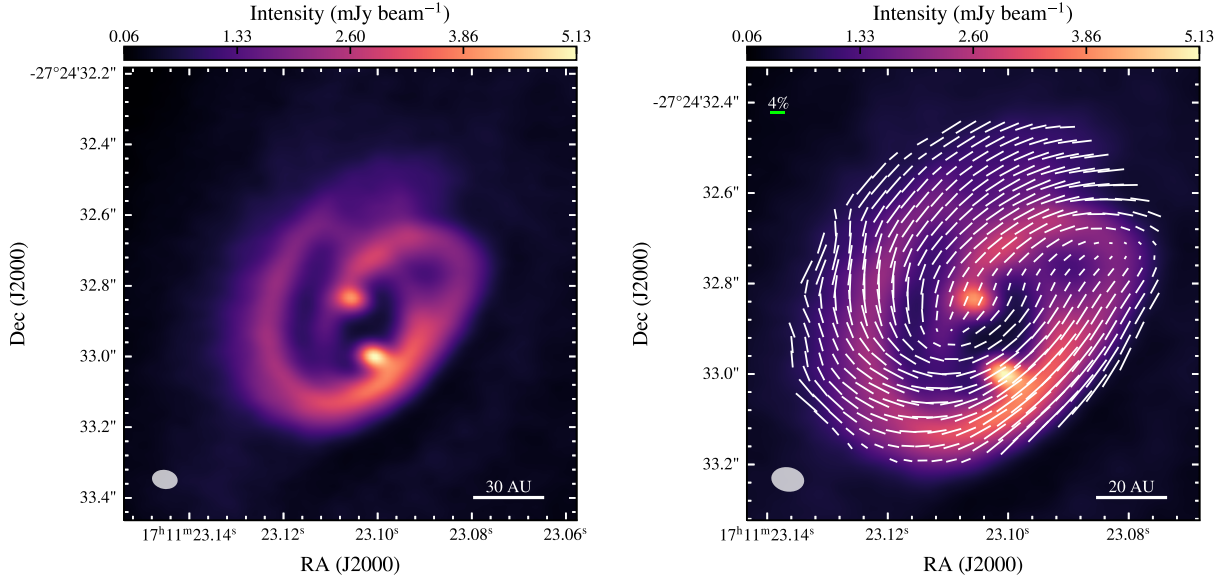


Figure 3: Left: A high-resolution ALMA Band 6 Stokes I map of BHB 07-11. The spiral arms can be seen clearly connecting the two sources in the binary. Right: The same high-resolution map with polarization vectors from the Band 6 data presented in Alves et al. (2018) overlaid on the spiral arms.

## 4 Science Goals

### 4.1 Identifying Polarization Mechanisms

If polarization is primarily induced by a mechanical alignment mechanism, polarization angles should be better aligned in high density regions of the circumbinary disk. Conversely, polarization alignment will be more pronounced in the low density regions if magnetic field alignment is prevalent. Thus, the proposed observations serve two purposes: identifying high density structure within the circumbinary disk, and identifying the polarization properties of such regions. Following the methods in Lin et al. (2024), we will use forward modeling to decompose the observed polarization morphology into its constituent components (mechanical, magnetic field, scattering) as was done with L1448-IRS3B (priv. comm.).

### 4.2 Alignment and Dust-Grain Properties

If mechanical alignment is prevalent within the disk, we can then identify specific properties of the alignment mechanism. Namely, we seek to identify whether the mechanism follows  $v$ -MET alignment as described in Hoang et al. (2022) or badminton-birdie alignment from Lin et al. (2024). It is also possible that both of these mechanisms could be prevalent in different parts of the circumstellar disk. Furthermore, we can also constrain dust grain shape, aspect ratio, degree of intrinsic polarization, and optical depth based on the properties of the alignment mechanism. Stephens et al. (2023), Lin et al. (2024). Additionally, we will use archival Band 4, 5, and 6 polarization-mode observations in the modeling process.

## 5 Analysis Plans

We will use the techniques described in Lin et al. (2022), Stephens et al. (2023), and Alves et al. (2018) to decompose the observed polarization morphology into its constituent components (mechanical, magnetic field, scattering) as was done with L1448-IRS3B (priv. comm.). If mechanical alignment is the prevalent mechanism, our models will be able to effectively constrain dust grain shape, aspect ratio, and optical depth within the circumbinary disk. Additionally, if magnetic field alignment is the dominant mechanism, we will be able to more effectively model the magnetic field and further constrain the strength of its components (toroidal, poloidal). Following Tu et al. (2024), we will also create MHD simulations of the system using ATHENA++ to further study the polarization mechanism within the circumstellar disk (Stone et al., 2020).

## 6 References

Alves et al. 2018, A&A, 616, 56 • Alves et al. 2019, Sci., 366, 90 • Harris et al. 2018, ApJ, 861, 91 • Hoang et al. 2022, ApJ, 164, 248 • Lin et al. 2022, MNRAS, 512, 23 • Lin et al. 2024, MNRAS, 528, 20 • Murillo et al. 2013, A&A, 560, 16 • Reynolds et al. 2021, ApJ Letters, 907, 33 • Sadavoy et al. 2018a, ApJ, 859, 15 • Sadavoy et al. 2018b, ApJ, 869, 14 • Sadavoy et al. 2024, A&A, 687, 16 • Stephens et al. 2023, Nature, 623, 3 • Tu et al. 2024, MNRAS, 532, 15

None Assigned

SG : 1 of 1      Science Goal      Band 7

VLA 1623!  
- Additional observations for the decomposition of poarization morphologies into constituent mechanisms (scattering, mechanical, magnetic).

Science Goal Parameters

| Ang.Res. | LAS  | Requested RMS | RMS Bandwidth          | Rep.Freq.      | Cont. RMS         | Cont. Bandwidth | Poln.Prod.  |
|----------|------|---------------|------------------------|----------------|-------------------|-----------------|-------------|
| 0.0400"  | 0.2" | 8 μJy, 54 mK  | 6681.853 km/s, 7.5 GHz | 336.500000 GHz | 7.97 μJy, 53.8 mK | 7.500 GHz       | XX,YY,XY,YX |

Use of 12m Array (43 antennas)

| t_total(all configs) | t_science(C-8) | t_total() | Imaged area | #12m pointing | 12m Mosaic spacing | HPBW   | t_per_point | Data Vol  | Avg. Data Rate |
|----------------------|----------------|-----------|-------------|---------------|--------------------|--------|-------------|-----------|----------------|
| 31.1 h               | 12.1 h         | 0.0 h     | 5.8 "       | 1             | offset             | 17.3 " | 43779.6 s   | 1857.0 GB | 24.6 MB/s      |

Use of ACA 7m Array (10 antennas) and TP Array

| t_total(ACA) | t_total(7m) | t_total(TP) | Imaged area | #7m pointing | 7m Mosaic spacing | HPBW | t_per_point | Data Vol | Avg. Data Rate |
|--------------|-------------|-------------|-------------|--------------|-------------------|------|-------------|----------|----------------|
|              |             |             |             |              |                   |      |             |          |                |

Spectral Setup : Single Continuum

| Center Freq (Sky) | Center Freqs. SPWs | Eff #Ch p.p. | Bandwidth   | Resolution | Vel. Bandwidth | Vel. Resolution | RMS                 |
|-------------------|--------------------|--------------|-------------|------------|----------------|-----------------|---------------------|
| 343.500000        | 336.500000         | 1920         | 1875.00 MHz | 2.258 MHz  | 1670.5 km/s    | 2.012 km/s      | 16 μJy, 108.0 mK    |
|                   | 338.500000         | 1920         | 1875.00 MHz | 2.258 MHz  | 1660.6 km/s    | 2.000 km/s      | 15.72 μJy, 104.9 mK |
|                   | 348.500000         | 1920         | 1875.00 MHz | 2.258 MHz  | 1612.9 km/s    | 1.942 km/s      | 16.34 μJy, 102.8 mK |
|                   | 350.500000         | 1920         | 1875.00 MHz | 2.258 MHz  | 1603.7 km/s    | 1.931 km/s      | 16.72 μJy, 104.0 mK |

1 Target

Expected Source Properties

| No. | Target     | Ra,Dec ( ICRS )     | V,def,frame --OR--z   |           | Peak Flux | SNR   | Linewidth | RMS (over 1/3 linewidth) | linewidth / bandwidth used for sensitivity | Pol. | Pol. SNR |
|-----|------------|---------------------|-----------------------|-----------|-----------|-------|-----------|--------------------------|--|------|----------|
| 1   | 1-VLA_1623 | 16:26:26, -24:24:29 | 0.00 km/s, hel, RADIO | Line      | 0.00 uJy  | 0.0   | 0 km/s    |                          |  | 0.0% | 0.0      |
|     |            |                     |                       | Continuum | 5.00 mJy  | 627.3 |           |                          |  | 3.0% | 18.8     |

Dynamic range (cont flux/line rms): N/A

**Justification for requested RMS and resulting S/N (and for spectral lines the bandwidth selected) for the sensitivity calculation.**

We use the archival Band 4 observations from 2018.1.00769.S, which were scaled to Band 7 using our proposed beam size of 0.04", as a guide for the spectral index. In Sadavoy et al. 2018a, Figure 5 shows a polarization fraction in the circumbinary disk of ~3%, which was used in the RMS calculation. At higher spatial resolution, however, polarization fraction is expected to increase due decreased beam smearing of the polarization vectors on the sky. Understanding the small-scale polarization morphology of the disk is critical to this project, as the orientation of the polarization vectors and the polarization fraction within the disk provide crucial information on the polarization mechanism(s) at work. To match Figure 1 in this proposal and Figure 5 in Sadavoy et al. 2018a we request an RMS of 8 uJy/beam.

**Justification of the chosen angular resolution and largest angular scale for the source(s) in this Science Goal.**

We seek to observe the small-scale polarization morphology within the circumbinary disk, and thus the chosen resolution of 0.04" is necessary. The density profile of the disk is directly related to the dominant polarization mechanism. Magnetic field alignment is expected to be greater in low-density regions, while mechanical alignment will be prevalent in high-density regions. The requested resolution will allow us to probe the densest portions of the disk and show whether polarization morphology is well aligned in these regions. The requested LAS of 0.2" will complement prior observations, as archival polarization-mode data (namely 2018.1.00769.S) have spatial resolutions between 0.181" and 0.295". We plan to combine our proposed observations with this archival data to fully map the polarization morphology within VLA 1623's circumbinary disk.

**Justification of the correlator set-up with particular reference to the number of spectral resolution elements per line width.**

In order to maximize continuum sensitivity we will use the default Band 7 properties. Additionally, we will use FDM mode to provide flexibility with any detected spectral lines in the continuum observations.

**Very High Imaging or Spectral Dynamic Range. Please explain why this is required and how it can be achieved.**

While Stokes I images have a high dynamic range, Stokes Q and U images do not. We expect that the Stokes Q and U maps will be ~3-4% of the Stokes I maps, meaning that high dynamic range will not be an issue, as the primary focus of the project is polarization.